PAPER

Check for updates

Cross-correlated humidity-dependent structural evolution of Nafion thin films confined on a platinum substrate†

Udit N. Shrivastava,[a] Kota Suetsugu,[b] Shusaku Nagano,[c] Helmut Fritzsche,[d] Yuki Nagao [ID][e] and Kunal Karan [ID]*[a]

Nanometer thin films of Nafion ionomer interfaced with platinum form the functional electrodes in many electrochemical devices including fuel cells and electrolyzers. To impart facile proton conduction in a Nafion ionomer, sufficient hydration of the Nafion ionomer is necessary to create a percolating network of water-filled nanometer-sized hydrophilic domains that manifest as macroscopic swelling. This hydration behavior of the ionomer thin films is poorly understood especially for films confined on electrochemically relevant Pt substrates. In this work, we present the evolution of hydration-dependent microscopic hydrophilic domains and macroscopic expansion of a 55 nm thin Nafion film on a Pt substrate. The cross-correlation among the film macro-expansion from ellipsometry, the micro-expansion from GISAXS, and the water distribution from neutron reflectometry (NR) explains the observed non-affine behavior of the film which can be attributed to the randomly and spatially non-uniform distribution of water domains. A correlation between the macroscopic factor (ε/τ) for protonic conductivity, and the domain size and swelling is presented for the first time. In addition, interfacial water between Pt and the ionomer interface is estimated at 75% and 84% RH, and an increase in domain size with RH is discussed to explain the increased activity and oxygen diffusivity with RH.

I. Introduction

Thin Nafion films are of technological importance to polymer electrolyte-based electrochemical devices such as fuel cells, electrolyzers, and sensors.[1–5] In the electrodes of these devices, sub-micron thin Nafion films coat the electron-conducting surface of the catalysts, such as Pt, to form an electroactive interface where their key function is to facilitate proton transport.[6–9] In addition, in the electrodes comprising ionomer-covered platinum, the reactants or analytes have to be transported through the ionomer films. Thus, the ionomer film controls both the local

ion conduction and the reactant transport through the film and to/from the electrochemical interface and influences the electrochemical performance parameters such as active area utilization and catalyst activity.[10,11] It is well known that the ionomer transport properties are a strong function of relative humidity (RH), which is a controllable operational parameter.[12,13] Pertinent to fuel cells, a recent study from Morimoto's group at Toyota Central R&D has demonstrated that the critically important transport resistances, *viz.*, the oxygen diffusion resistance across the Nafion thin film and the interfacial resistance at the buried interface (*i.e.* at the Pt/ionomer interface), decrease significantly with RH.[14]

These hydration-dependent transport properties are a manifestation of a key microscopic structural feature of these ionomers – the hydrophilic ionic domains formed by clustering of the sulphonic acid ($SO_3^-H^+$) ion-pairs distributed in the hydrophobic fluorocarbon matrix. In fact, much of the research on the structure of the membrane form of Nafion has been focused on the size/shape of these ionic domains using small angle X-ray scattering (SAXS) studies.[12,13]

However, thin films are fundamentally different from bulk membranes due to the confinement effects and the interfacial interaction induced orientation of ionomer chains resulting in anisotropic structures and properties.[15,16] The literature on

[a] *Department of Chemical and Petroleum Engineering, University of Calgary, Calgary, AB, Canada. E-mail: kkaran@ucalgary.ca*

[b] *Department of Molecular and Macromolecular Chemistry, Graduate School of Engineering, Nagoya University, Furo-cho, Chikusa, Nagoya 464-8603, Japan*

[c] *Nagoya University Venture Business Laboratory, Nagoya University, Furo-cho, Chikusa, Nagoya 464-8603, Japan*

[d] *Canadian Nuclear Laboratories, Chalk River, ON, Canada*

[e] *School of Materials Science, Japan Advanced Institute of Science and Technology, 1-1 Asahidai, Nomi, Ishikawa 923-1292, Japan*

† Electronic supplementary information (ESI) available: The difference between volumetric and thickness expansions from cycle-to-cycle. Fits on GISAXS data (intensity *vs.* scattering vector). Method to estimate the volume fraction from the NR-SLD. Fitting of the NR data and all the fit parameters to validate the selection of the model shown in the main paper. See DOI: 10.1039/c9sm01731c

Nafion thin films on SiO_2 has provided sufficient evidence of thickness-dependent water uptake, proton conductivity, ionomer wettability, modulus of elasticity, thermal expansion and micro-to-macro relationship (local domain size-to-hygro-expansion).[17–27] In addition to confinement, interaction with a substrate can strongly influence the structure of thin films resulting in substrate-dependent macroscopic and microscopic properties.[28–34] For example, substrate-dependent layered morphology and orientation of hydrophilic domains within hydrophilic domains have been observed using scattering techniques such as neutron reflectometry (NR) and grazing incidence small angle X-ray scattering (GISAXS).[30–34] Substrate-dependent macroscopic properties such as water uptake kinetics, proton conductivity, and thermal expansion of the films have also been reported.[24,25,34] Macroscopic properties of ionomer thin films on Pt such as proton conductivity, and the microscopic structure such as water distribution and ordering of hydrophilic domains greatly differ from those of the ionomer thin film on SiO_2.[24,30,31] In other words, macroscopic properties and the likely microscopic structure of thin Nafion films not only differ from those of the bulk membrane but also are substrate-dependent.

Insofar as the microscopic structure – the ionic domain – is concerned, a hydration-dependent d-spacing derived from the so-called ionomer peak in SAXS data provides an insight on the size of the hydrated domains.[22,36] For Nafion thin films, the GISAXS measurements have shown anisotropic character (in-plane *vs.* out-of-plane) of the ionomers.[22,30] Both confinement and interaction with the substrate can induce hydration-dependent non-uniform spatial distribution of d-spacing. Although SAXS is a very powerful tool in determining the size of micro-domains, it does not provide information on the spatial distribution of the d-spacings or on their spatial configuration and connectivity. This adds to the complications in correlating the macroscopic changes, *i.e.* the swelling of films with the changes in the microscopic structural parameter, *i.e.* the ionic domain-related d-spacing. Furthermore, the commonly employed methods for determining the macroscopic hydration property of ionomer thin films, *viz.*, ellipsometry and quartz crystal microbalance (QCM) fundamentally measure different characteristics. Ellipsometry measures the overall thickness change of polymers, whereas QCM measures the total mass change. Often the analyses consider that the dry polymer volume and water volume are additive to yield the observed change. Such an assumption neglects any changes in the density of the hydrophobic matrix upon water sorption in the hydrophilic ionic domains. Ideally, the volume change (ΔV) determined from swelling measurements should compare with that estimated from mass change. However, if the polymer plasticizes, and its elastic property changes with hydration, swelling-based water uptake may not equate to gravimetric mass uptake. A previous study on Nafion thin films coated on Au showed a higher ΔV estimated from mass uptake measured using QCM than ΔV calculated from swelling measurements using ellipsometry.[27] Furthermore, it is unlikely that interfacial water on a realistic (non-atomistic smooth) surface will contribute to the swelling of the ionomer. Our recent NR study has shown that a significant amount of water can be present at the Pt/ionomer interface.[34] As alluded to above, NR studies have also shown

non-uniform distribution of water through the thickness of the Nafion film.[31] Thus, it may be expected that the number density and/or the size of the hydrated domains may vary across the thickness of the films. Therefore, it is not obvious whether the microscopic parameter (d-spacing) would linearly correlate with the macroscopic parameter (swelling).

The review of the literature reveals that, in general, there has been only a very limited effort to correlate the macroscopic properties of the ionomer thin films with its microscopic structure. So far only one study reports the relationship between the macroscopic and microscopic expansions of thin films on SiO_2, where a $\sim$50 nm thin film follows affine behavior *i.e.* macroscopic expansion 1:1 correlates with microscopic expansion.[22] However, given the significant differences in macroscopic properties of Nafion thin films on SiO_2 and on Pt, the microscopic–macroscopic property relationship presented for the films on SiO_2 cannot be assumed to be applicable for films on Pt.[5,22]

This study is a first report wherein the hydration behavior of an $\sim$55 nm Nafion thin film on an electrochemically relevant Pt substrate is cross-correlated with multiple techniques – ellipsometry, quartz crystal microbalance, GISAXS, and neutron reflectometry – examining the structure and/or properties at multiple-length scales. Simultaneous measurements of hygro-expansion (by ellipsometry) and mass water uptake (by quartz crystal balance or QCM) on the same sample over a range of relative humidity were carried out. The results demonstrate a systematic difference in water contents estimated from the two methods, which may have implications for a majority of the literature data on perfluoro sulfonic acid (PFSA) thin films obtained from ellipsometry. The RH-dependent microscopic structures, *viz.* the hydrophilic domains from GISAXS and the water distribution using NR were measured. GISAXS results provide evidence of in-plane domain expansion opening up the possibility of in-plane film expansion, which has typically been neglected in the literature. NR measurements show non-uniform distribution of water in the out-of-plane direction, which raises the question about the relevance of using a single-value of d-spacing (derived from the ionomer peak of GISAXS data) to characterize the microscopic structure. Finally, the microscopic (d-spacing) and macroscopic (water volume fraction) hydration parameters are correlated to the structural factor (phase volume/tortuosity or ε/τ) for proton conductivity using conductivity data for an $\sim$50 nm Nafion film reported in an earlier study.[23] The implications of the hydrated microstructure on electrochemical activity and oxygen transport are also discussed.

II. Experimental

A. Sample preparation

Two different Pt substrates were employed: a Pt-electrode of a QCM crystal (Inficon, USA) and a sputter-coated Pt film on a SiO_2 substrate. A 1.7 wt% dispersion of EW1100 was prepared by adding an appropriate amount of isopropyl alcohol (IPA) to a stock solution. The Nafion dispersion was spin coated on the Pt substrates and dried in a vacuum for 24 hours at 40 °C.

B. Combined QCM-ellipsometry

An environmental cell was designed to accommodate the QCM holder and to control both RH and temperature. Humidified air was flowed through the cell and desirable RH was obtained by mixing a fully humidified gas stream with a dry gas stream. Upon change in RH direct mass uptake of water in the film was measured as a frequency change (Stanford Research Science Instruments) and simultaneously the change in film thickness was measured using an ellipsometer (M2000, JA Woollam, USA).

C. RH dependent contact angle

A goniometer is used to measure contact angle at controlled RH using a salt solution and temperature in an environmental chamber (Rame Hart Inc., NJ, USA).

D. Water distribution in thin films as determined by NR

Thin films coated on Pt films were employed for NR measurements at the National Research Universal (NRU) reactor at the Canadian Nuclear Laboratories in Chalk River, Canada. Details on the used sample cell can be found elsewhere.[37] Salt solutions were used to maintain specified RH and the cell was immediately exposed to ambient RH every time before the salt solution was changed. A typical NR measurement took 8–12 hours.

E. RH dependent GISAXS

GISAXS measurements were taken with a Rigaku FR-E X-ray diffractometer with an R-AXIS IV two-dimensional (2D) detector and Cu Kα radiation (λ = 1.542 Å). Voltage of 45 kV, current of 45 mA, and irradiation time of 10 min were applied with a beam size of approximately 300 μm × 300 μm and a camera length of 300 mm. Samples were placed into a humidity-controlled cell with X-ray transparent polyester film (Lumirror) windows. Nitrogen carrier gas was used as received from the gas cylinder without further dehumidification to control the humidity. X-ray scattering patterns were recorded on an imaging plate (Fujifilm Corp.). The incident angle was chosen as 0.20–0.22°.

For out-of-plane and in-plane profiles, the integrated regions were taken between $-0.5°$ and $+0.5°$ as 2θ from the center $(0°)$ and the width of $1°$ as 2θ, respectively.

III. Result and discussions

A. Swelling and water mass uptake

A small difference in water volume fraction (ϕ_w) in ~ 50 nm Nafion film on gold from mass uptake (QCM) and swelling (ellipsometry) was reported in a previous study, co-authored by one of the authors of the current study.[27] In the previous work, two separate samples were used for QCM and ellipsometry. Thus, there has been a lingering question as to whether the observed difference is due to sample to sample variation or a real phenomenon. To eliminate the sample-to-sample variation issues, in this work, humidity-dependent hydration behavior of a ~ 54 nm thin Nafion film on the Pt surface of a QCM electrode was simultaneously measured by QCM that yielded mass uptake (Δm, accuracy ± 17 ng cm^{-2}) and by ellipsometry which yielded swelling (ΔL, accuracy ± 1 Å), respectively. In a separate experiment, using ellipsometry, the swelling of a ~ 54 nm thin Nafion film on a 10 nm thick Pt/SiO$_2$/Si substrate was measured, as well. Assuming that the hydrophobic matrix density remains unchanged upon hydration of ionic domains, the volume of hydrated ionomer is equal to the volume of dry polymer plus the volume of water sorbed by the ionomer at a given RH. Thus, the mass uptake and swelling can be converted to water volume fraction (ϕ_w) in the hydrated polymer as reported and compared in Fig. 1a. The inset in Fig. 1a shows the water uptake on the bare Pt substrate as a function of RH. In the case of QCM, to estimate water volume fraction the mass of sorbed water on the bare Pt was deducted from total mass of water absorbed by the Nafion thin film.

In a separate experiment, neutron reflectometry measurement on a film of similar thickness was also performed and is discussed in detail in a later section. Data fitting of the NR results yields two parameters – film thickness and the scattering
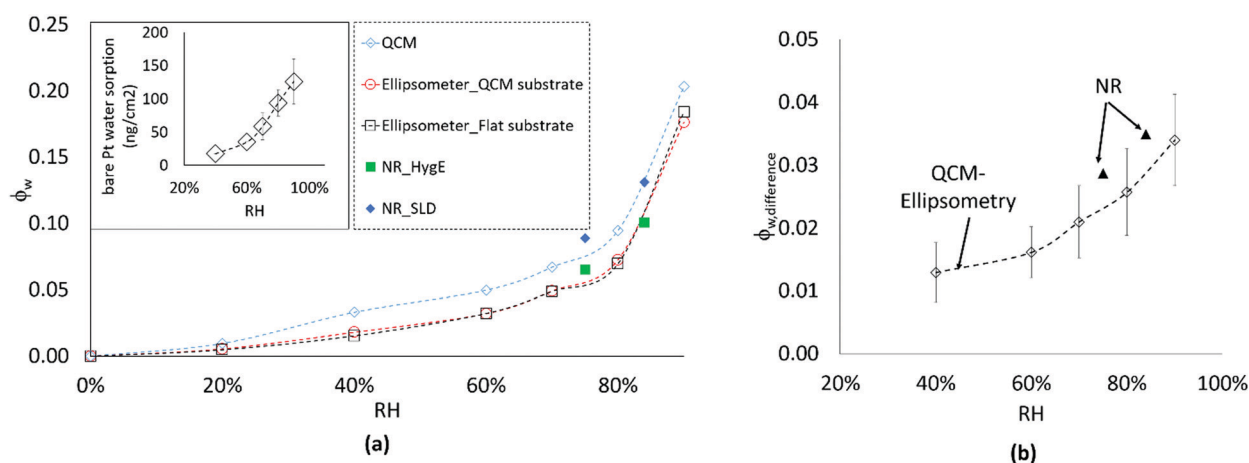

Fig. 1 (a) Estimated ϕ_w from QCM, ellipsometry and NR measurements; NR_HygE and NR_SLD are volume fractions estimated from NR–data fitted film thickness and SLD, respectively, of wet and dry films; inset shows mass of water sorbed by bare Pt. (b) The differences between ϕ_w values estimated from QCM and ellipsometry data plotted as a function of RH.

length density (SLD). The thickness and SLD of the dry and the hydrated films independently yield water volume fractions and are denoted as NR_HygE and NR_SLD water volume fraction, respectively, and are shown in Fig. 1a. The differences in ϕ_w estimated from three different ionomer coated Pt samples, investigated by three different techniques: (a) mass uptake from QCM using the Sauerbrey equation (b) swelling from ellipsometry and NR data fitting (c) volume fraction from the difference in the SLD of dry and hydrated (wet) films, are quite noticeable. The difference in ϕ_w from QCM and ellipsometry is denoted by $\phi_{w,difference}$ and plotted in Fig. 1b. Although QCM and ellipsometry derived ϕ_w were obtained from different areal sizes examined in the two techniques, *viz.* 1 cm^2 for QCM and $\sim$0.36 cm^2 for ellipsometry, they compare very well with NR-derived volume fractions obtained from the SLD and the thickness (NR_SLD ϕ_w and NR_HygE ϕ_w), respectively. This strongly supports the observation that the differences in water volume fractions obtained from the swelling and water uptake data, even if small, are real and significant.

The simultaneous measurements of swelling and mass uptake of water rules out the sample-to-sample variation. It is possible that the $\phi_{w,difference}$ arises from an unaccounted systematic error. We also cannot rule out if this difference arises from a physical phenomenon such as compression or densification of the hydrophobic backbone, which is not considered when assuming that the polymer matrix density remains unchanged. Resolving the origin of this discrepancy would require further specialized measurements such as positron annihilation spectroscopy, which can provide information on free volume change but is outside the scope of this work.

All the equations pertaining to the calculation of water volume fraction are presented in the ESI.† The changes due to RH cycling is also reported for one sample that was cycled three times between 0% and 90% RH, showing a systematic difference in water volume fractions computed from hygroexpansion and mass uptake analyses for each cycle (Fig. S1 of ESI†), even if the swelling varies slightly from cycle-to-cycle. This further highlights the technique-dependent difference in water content estimation. Both ϕ_w and $\phi_{w,difference}$ increased steadily with RH and a sharp increase in both is observed after 80% RH where ϕ_w from QCM is almost 10% of the total volume. Evidently, from Fig. 1a, most of the water uptake is due to the swelling of the film in the out-of-plane direction, which is expected as the film is confined, and strongly interacting with Pt.[30]

B. Microscopic–macroscopic expansion

To further our understanding of hygro-expansion of the film, we analyzed the GISAXS results to relate micro-structure to macroscopic swelling. RH dependent GISAXS response of the film was measured from 5% to 90% RH; examples of GISAXS patterns are presented in Fig. 2a, I–IV. From the 2D profiles both out-of-plane (OP) intensities (I_{op}) and in-plane (IP) intensities (I_{IP}) were derived and plotted against the scattering vector (q, nm^{-1}) in Fig. 2b. With increasing RH, the corresponding water uptake increases, and there is both an increase in the scattering intensity and a shift of the scattering peak towards the lower q.

The d-spacing, obtained from the peak position, as a function of RH is plotted in Fig. 3. Whereas a discernable change in OP d-spacing with RH is noticeable for the whole range (20–90% RH), the IP d-spacing change was quantifiable only above 60% RH (fits are presented in Fig. S2 of ESI†). Upon extrapolation, the OP d-spacing (2.5 nm) in the dry state of the Nafion thin film on Pt is very close to the d-spacing (2.7 nm) of dry membrane.[21] Furthermore, at similar water content ($\lambda \sim 7$), the OP d-spacing (3.2 nm) of the thin film on Pt is 11% lower than the overall
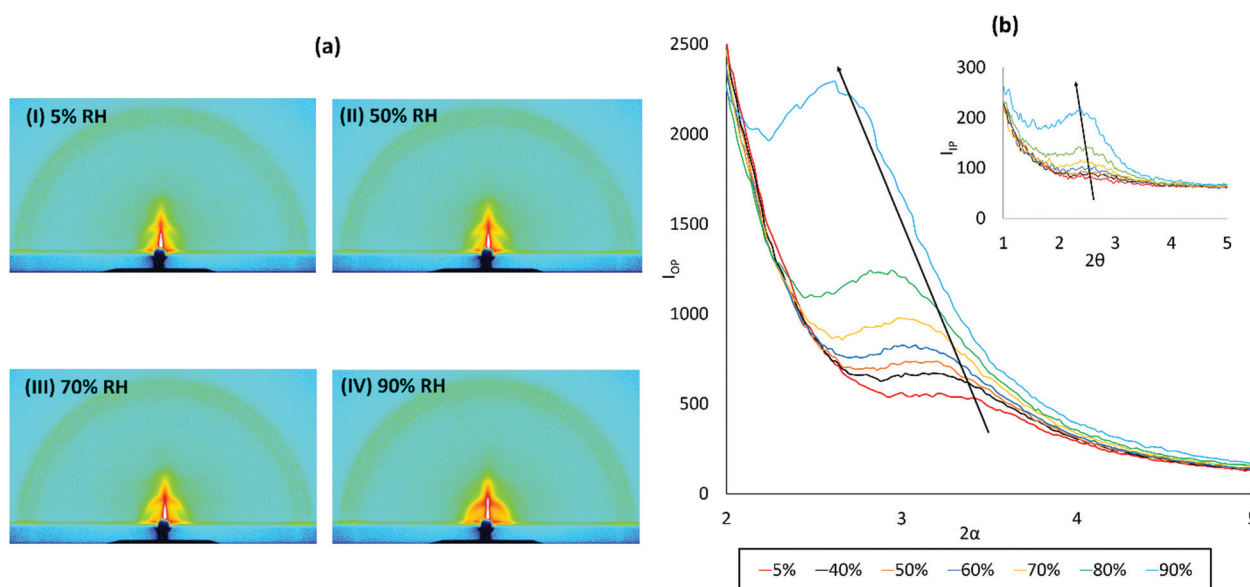

Fig. 2 GISAXS measurements for a 54 nm Nafion (EW 1100) film on Pt equilibrated at various humidities. (a) GISAXS patterns at (I) 5% RH, (II) 50% RH, (III) 70% RH, and (IV) 90% RH. (b) Intensity as a function of scattering vector from 5% RH to 90% RH; inset shows IP intensity *vs.* scattering vector.
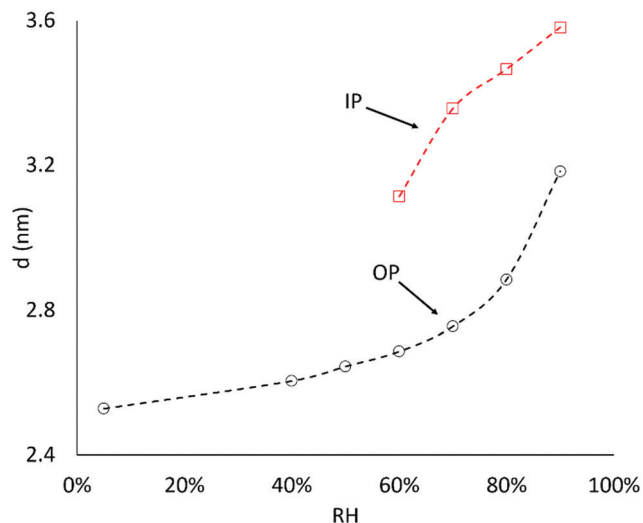
Fig. 3 Microscopic and macroscopic swellings as a function of relative humidity for 54 nm thick Nafion (EW1100) coated Pt at 25 °C, out-of-plane (OP) and in-plane (IP) d-spacings obtained from analyses of GISAXS data (Fig. S2 in ESI†).

d-spacing (3.6 nm) of the membrane, while it matches with OP d-spacing of 50 nm Nafion thin film on SiO$_2$.[21]

A shift in I_{IP} to lower q with increasing RH indicates that the d-spacing in the IP-direction is increasing. Confinement effects and/or strong interaction of the ionomer with the substrate would both result in restricted mobility in the IP direction; yet, the film is free to expand in the OP direction. This could explain the noticeable expansion of the OP component of the domains at RH of up to 60% but correspondingly small expansion of IP component. Also, the d-spacing in the IP direction is larger than that in the OP direction. Considering these results, it may be deduced that both, confinement and interaction of ionomers with Pt are responsible for the constrained expansion in the IP direction at low RHs but once domains are filled with sufficient water, the plasticization of the polymer allows the IP expansion. d-Spacing can increase due to the expansion of the matrix and/or of the water-filled hydrophilic domains. Furthermore, Kusoglu *et al.*, reported an increase in nanoscopic swelling of domains in the IP direction for a Nafion thin film on SiO$_2$.[21] In their work, coalescence of the IP domains was presented as a hypothesis to explain local swelling of nanoscopic domains. It has also been argued that the $\phi_{w,\text{difference}}$ may arise from the in-plane expansion of films.[27] There is a possibility of an in-plane expansion due to the microscopic swelling. However, in the absence of direct evidence, IP domain expansion cannot be used as a concrete proof of in-plane expansion and, by extension, it cannot be established with certainty that $\phi_{w,\text{difference}}$ arises from in-plane expansion.

Kreuer and Kusoglu correlated swelling with domain expansion for different PFSA membranes along with various treatments and asserted that their structure is locally flat.[11,21,36] However, d-spacing in itself is not sufficient to provide insight on correlation between microscopic structure and macroscopic structure. For instance, membranes and thin films thicker than 100 nm show non-affine ($\Delta d/d_{\text{dry}}:\Delta L/L_{\text{dry}} \neq 1:1$) behavior, meaning local domain expansion does not correlate 1:1 with overall swelling – a clear explanation of this phenomenon is still lacking.[11] Nonetheless, 55 nm thick Nafion thin films on SiO$_2$ substrates have been reported to exhibit affine behavior. Here, a similar analysis is performed and the relative change of the domain size in the OP direction is computed and correlated with the swelling in the OP direction (from ellipsometry). To compute Δd, we reference the OP domain size (d_z) at 0% RH estimated by extrapolation of (d_{OP}) *versus* RH data. The relative changes in domain size plotted against corresponding changes in macroscopic expansion for the films are shown in Fig. 4a and a non-affine behavior is clearly noted. Up to 80% RH, similar to previously reported data for Nafion membrane and Nafion film thicker than 100 nm on a SiO$_2$ substrate, a linear correlation between $\Delta d_{\text{op}}/d_{\text{op,dry}}$ and $\Delta L_{\text{op}}/L_{\text{dry}}$ is noted but the $\Delta d_{\text{op}}/d_{\text{op,dry}}:\Delta L_{\text{op}}/L_{\text{dry}}$ ratio is $\sim 2:1$. For RH between 80% and 90%, this ratio is close to 1:1 indicating affine behavior. Compared to membranes and thick ionomer films where polymer mobility is higher than in a film confined to a substrate and possibly strongly interacting with the substrate since sulfonic groups are known to have strong interaction with Pt,[33,35] the domains are expected to be aligned parallel to the Pt[30] and should result in affine behavior but that is definitely not the case. Both macroscopic water volume fraction and microscopic domain size are essentially average quantities and possibly non-uniformly distributed within the confined ionomer thin film. Moreover, a thin film confined to the substrate also has a certain orientation order which changes with RH.[28] Thus, it is not essential that changes in a single microscopic parameter, d-spacing obtained from GISAXS data, may necessarily exhibit an affine relationship with macroscopic changes.

The area under the I–q Gaussian curve is proportional to the volume fraction of scatterers[36–38] and for a locally flat thin film the Gaussian area is expected to be proportional to swelling – which is the case (see Fig. 4b). In a homogeneous/isotropic ionomer material, all the ionic domains would have nearly equal water content. Thus, the number of scatterers does not change but their size and correspondingly the volume fraction of the scattering entities increase with increasing hydration. On the other hand, ionomer thin films can be anisotropic and are known to exhibit a layered structure with varying water contents through the thickness of the film. In other words, the domains may be unequally hydrated. Thus, in essence, the effective number of scatterers will be changing with hydration. An integrated value of intensity with respect to q-vector would account for changes in the number of scatterers.

In our experiments, at 5% RH a small peak has been observed in the q-range typically attributed to the 'ionomer peak' indicating that at least some of the domains may be sufficiently hydrated. With an increase in RH, both the peak intensity and its position are expected to change. The integrated area correlates linearly with macroscopic expansion (ΔL), suggesting that the non-affine behavior of the ionomer film most likely arises from non-uniform spatial distribution of water within the film.

For RH-dependent water distribution in the OP direction, we examined the neutron reflectometry (NR) data at 8%, 75%, and 84% in an H$_2$O environment. The reflectivity response was
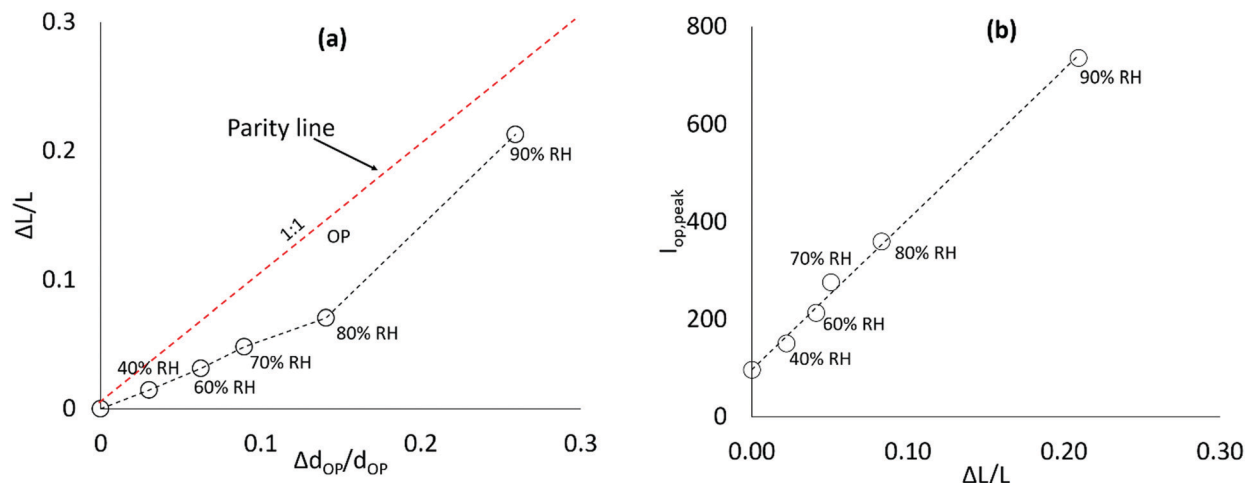
Fig. 4   (a) Comparison of macroscopic expansion with microscopic expansion in the OP direction. (b) GISAXS ionic domain OP peak area as a function of swelling or OP macroscopic expansion.

fitted with a four-layer model (Table S1 in the ESI† describes the quality of the fit). At dry conditions (8% RH), a single layer with uniform SLD was found to be sufficient to describe the NR response from the Nafion film structure, while at higher RHs a multi-layer model, as described below, was needed to fit the data (all the fits with NR data are shown in Fig. S3, ESI†). The corresponding SLD profiles are shown in Fig. 5a.

The multi-layer description of the ionomer film comprises of three layers with uniform SLD and two gradient layers with an error function like SLD profile. The layered model comprises of: (i) an interfacial layer in contact with Pt, which is a mix of water and polymer; the SLD of this layer is lower compared to the SLD of dry (8% RH) film because the SLD of H_2O is $-0.056 \times 10^{-5}\,\text{Å}^{-2}$; (ii) an inner layer, which is the driest layer within the film and its SLD approaches that of the dry polymer; (iii) a gradient layer wherein the SLD transitions from that of the dry inner layer to that of the

wetter outer layer; (iv) an outer layer with the lowest SLD, implying that most of the water is accumulated in this layer; (v) a hydrophobic surface layer where SLD approaches that of the SLD of the dry layer; noticeably this hydrophobic layer persists even when the film is exposed to RH as high as 88% for 24 hours, in Fig. 5b, the contact angle presents strong evidence of such a surface layer.

The overall physical description of the Nafion thin film is supported by external evidences: (1) water sorption at bare Pt is an indirect evidence of water at the Pt–ionomer interface, (2) $\phi_{w,\text{difference}}$ estimated from NR model-based SLD and swelling is similar to $\phi_{w,\text{difference}}$ from QCM and ellipsometry, and (3) the presence of a hydrophobic skin layer from the model also described by the contact angle measurements. The hydrophobic surface of Nafion is well known and is discussed in a recent article by Karan.[5] There is evidence of a skin layer from GI-SAXS and GI-XRD studies of Nafion films.[40,41]
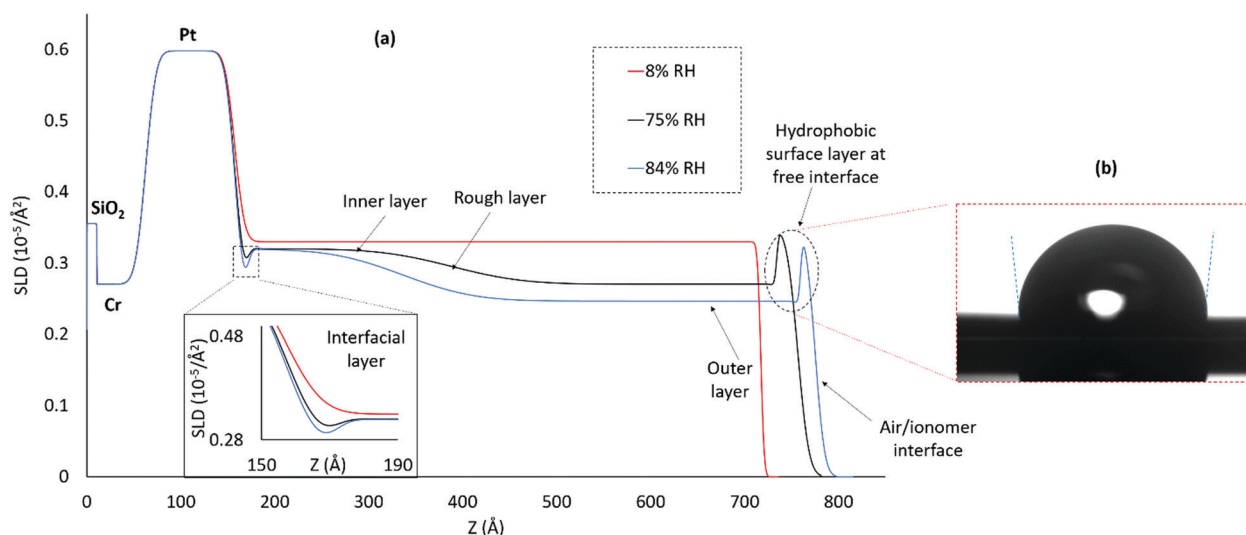

Fig. 5   (a) SLD profiles of Nafion film on Pt at different relative humidities (H_2O environments) at 25 °C; a zoomed SLD profile of Pt/ionomer interface region is shown as an inset. (b) An image of water contact angle measured at the surface of ionomer at ~88% RH.

Using eqn (S5) of ESI,† SLDs were converted to water volume fraction. As RH increases from 75% to 84%, the ϕ_w in the 1.4 nm thick interfacial layer at the buried interface (see SLD profiles in Fig. 5a) increases from 20% to 26% indicating humidity-dependent interfacial water. Beyond the interfacial layer, a dry layer exists near the interface with $\phi_w \sim 3\%$ at both RHs; however the thickness of the dry inner layer reduces from 26 nm to 17 nm as RH increases from 75% to 84%, and the roughness of the inner layer remains the same 6 nm, which translates to a 24 nm thick gradient layer. In a similar fashion, the thickness of the wet outer layer increases from 30 nm to 42.5 nm, whereas ϕ_w increases slightly from $\sim15\%$ to $\sim21\%$. In either case, a rough hydrophobic surface layer or skin layer persists at 75% RH and at 84% RH. In a separate experiment using a special environmental chamber, similar films on Pt were exposed for 18 hours to 75% and 84% RHs (*i.e.*, similar to the conditions of the NR experiments) and the water contact angle of $\sim90°$ was found (see the image in Fig. 5b). It is quite intriguing that the nature of the surface is independent of RH. In fact, Kawamoto *et al.* report a similar RH-independent surface layer for ionomers coated on a Si substrate.[39] Even though NR measurements could not be performed at all the RHs, it provides sufficient evidence of spatial distribution of water within the ionomer coated on Pt. Thus, the non-affine behavior is likely to originate from spatial distribution of the water. To elaborate, one of the reasons put forth for suppressed water uptake in thin films compared to thicker films and membranes is the idea of higher elastic modulus of the polymer for thinner films.[5,16] Due to the higher elastic modulus, higher mechanical forces exerted by the hydrophobic matrix counteract the chemical force for hydration resulting in a lower water uptake. A gradient in elastic modulus can be expected for Nafion films on platinum. The polymer near the substrate has arguably higher elastic modulus due to strong interaction with the Pt substrate compared to the polymer away from the Pt/ionomer interface. Thus, the gradient in water distribution is most likely to originate from the gradient in the elastic modulus from the buried interface to the surface of the ionomer.

C. Conductivity–structure correlation of ionomer thin film on Pt

Ono *et al.* have reported conductivity measurements (σ in S cm^{-1}) of a ~50–55 nm thin film on Pt in an earlier study.[23] The water content, λ (# of water molecules/sulfonic molecule) of a 55 nm film can be deduced from the mass uptake measured by QCM in the present work:

$$\lambda = \frac{M_{RH,ion} - M_{dry,ion}}{M_{dry,ion}} \cdot \frac{EW \cdot \rho_w}{\rho_{ion} \cdot M_w} \qquad (1)$$

where, $M_{RH,ion}$ is the RH-dependent mass of the ionomer film, $M_{dry,ion}$ is the mass of the dry ionomer film, EW is the equivalent weight, ρ_w is the density of water, ρ_{ion} is the density of ionomer, and M_w is the molecular weight of water.

It can be noted from the data in Fig. 6a that σ increases by two orders of magnitude from 40% to 90% RH and λ increases steadily till 80% RH and then sharply increases between 80% RH and 90% RH. It is common to correlate the proton conductivity σ with λ. It is obvious from Fig. 6b that at $\lambda < 4$, conductivity is very sensitive to water content. For instance, λ increases by 2 between 40% and 80% RH but σ increases by orders of magnitude and then four times till $\lambda \sim 8$. It should be noted that λ is an average value computed from the overall water volume or mass fraction and does not take into account the OP water distribution. These average lambda values indicate the average local chemical environment of the sulfonic groups *i.e.* the amount of water molecules attached to a sulfonic group which can dictate the water transport mechanism.

For PFSA membranes, Kusoglu *et al.* identified an empirical relationship among conductivity (σ), water content (λ), and domain spacing (d), and that is $\sigma \propto \dfrac{\lambda}{d}$.[21] However, by accounting structural properties such as volume fraction of water-filled
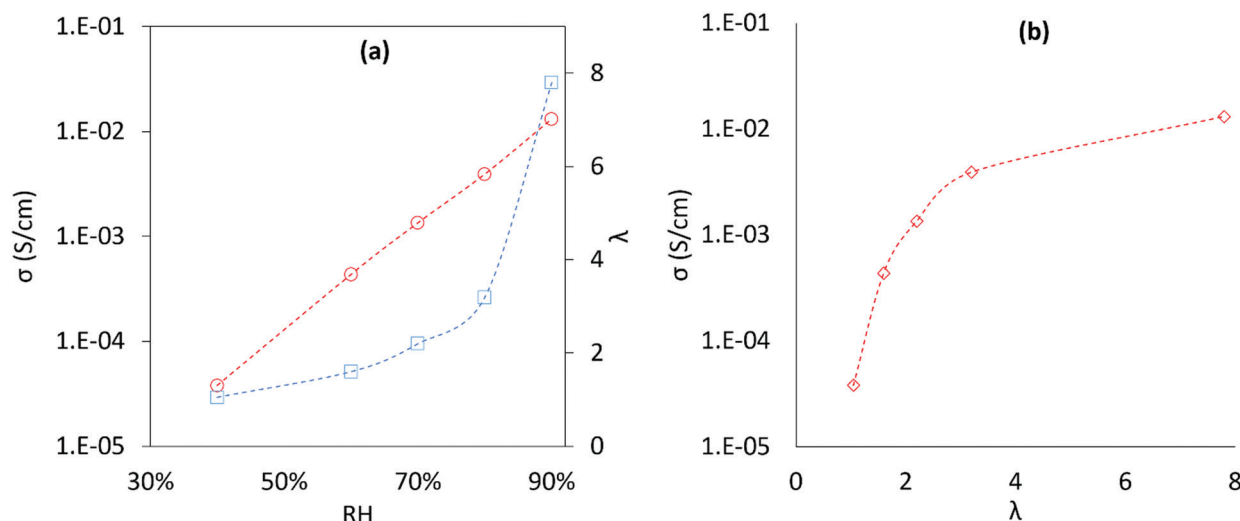

Fig. 6 (a) Conductivity (red circle)[23] and water content (blue squares) [this work] of ~50–55 nm ionomer thin film on Pt at 30 °C. (b) Conductivity as a function of water content at 30 °C.

domain-proton transport (ε) and tortuosity of pathways (τ) for the long-range transport of protons, the generic form of conductivity of protons in an ionomer thin film or membrane in terms of proton concentration (C_{H^+}) and proton mobility (μ_{H^+}) is commonly expressed as:

$$\sigma = [C_{H^+}\mu_{H^+}]\left[\frac{\varepsilon}{\tau}\right] \qquad (2)$$

Choi et al. developed a model to compute the proton conductivity of Nafion membrane.[42] In particular, their model accounted for the water content (λ)-dependent mobility and concentrations of protons by considering surface and bulk (comprising the Grothuss and free water) transport within the connected network of hydrophilic ionic domains. The commonly used epsilon–tau (ε/τ) model was adopted considering the composite nature of the ionomer accounting for the volume of the conducting phase (ε) and tortuous pathways of the conducting phase (τ). The conductivity equation proposed by Choi et al.[42] is shown below:

$$\sigma = (\varepsilon/\tau)\cdot\left[\frac{F^2}{RT}\left(D_{H^+}^{\Sigma}C_{H^+}^{\Sigma} + D_{H^+}^{G}C_{H^+} + \frac{D_{H^+}^{W}C_{H^+}}{1+\delta_c}\right)\right] \qquad (3)$$

where, F is the Faraday constant, R the universal gas constant, T the temperature, $D_{H^+}^{\Sigma}$ the surface proton diffusivity, $D_{H^+}^{G}$ the Grothuss proton diffusivity, $D_{H^+}^{W}$ the vehicular proton diffusivity, $C_{H^+}^{\Sigma}$ the concentration of surface protons, C_{H^+} the concentration of exchanged protons, and δ_c is the diffusion coefficient ratio. Here, the term within square brackets can be thought of as the intrinsic conductivity of the protons within the ionic domains and is the function of λ only. It can be argued that the differences in the observed conductivities between a thin film and bulk ionomer at a given λ are attributable to the microstructural parameters (ε/τ). The parameter ε is equivalent to ϕ_w. Below $\phi_w \sim 0.2$, Kreuer et al. found highly suppressed proton conductivity but almost similar to water diffusivity in the Nafion membrane which indicates that the vehicular mechanism dominates the proton transport in membranes.[43] For the conductivity measurements reported on 50 nm Nafion film by Nagao's group, the water volume fraction (ϕ_w) is below 0.2. Hence, vehicular mechanism is assumed as the primary mechanism of the proton transport, which simplifies the form of eqn (3) to:

$$\sigma = (\varepsilon/\tau)\left[\frac{F^2}{RT}\left(\frac{D_{H^+}^{W}C_{H^+}}{1+\delta_c}\right)\right] \qquad (4)$$

Kreuer et al. compared the microstructural domain sizes, water diffusivities, and proton conductivities among polyaryl hydrocarbon and Nafion membranes.[43,44] In their work, polyphenylene and Nafion membranes exhibited comparable diffusivity at similar λ but hydrophilic domains in polyphyenylene were measured to be smaller than that of Nafion – indication of weak correlation between domain size and intrinsic conductivity. Yet, at a similar volume fraction proton conductivity of the polyphenylene membrane was much lesser than that of Nafion.[43] Similarly, a sulfonated-poly ether ketone membrane with a much smaller domain size than that of Nafion, which results in highly tortuous and dead end domains, showed relatively much lower water

diffusivity and conductivity at the same volume fraction.[44] Observations from these papers are indicative of domain size relevance to the structural parameters. Therefore, as the film expands, both, an increase in domain size and water volume fraction lead to the development of more proton conducting pathways, and tortuosity is expected to fall. A linear relationship between structural factors (ε/τ) computed from eqn (3) with product of water volume fraction and domain expansion $\phi_w\Delta d_{op}$ is identified (Fig. 7). Furthermore, since, ϕ_w is equal to ε, the tortuosity of proton-conducting domains can be computed. It is found that the tortuosity is inversely proportional to the domain expansion (see inset in Fig. 7).

D. Implications to oxygen transport resistance and Pt poisoning

Oxygen transport resistance across the ionomer thin film and Pt poisoning owing to adsorption of sulfonic groups are relevant to the performance of fuel cells. A recent report from Morimoto's group have clearly pointed out that Pt poisoning occurs mainly due to the adsorption of sulfonic groups at a Pt site. The degree of adsorption or poisoning strongly depends on the amount of interfacial water (water at the Pt/ionomer interface) which increases as RH increases resulting in more sulfonic group desorption.[45] Evidently, NR data from the present study show that the ϕ_w at the interface increases from 20% to 26% as RH increases from 75% to 84% and in a previous NR study from our group,[33] at 97% RH two monolayers of water at the Pt–ionomer interface separating ionomer from Pt were found. Consequently, water has a major role in reducing the Pt poisoning, mechanism of which is replacement of sulfonate groups by water.

In another study from Morimoto's group, in an ex situ experiment it was found that the estimated interfacial resistance for oxygen transport and diffusivity of oxygen through thin film decreases with RH. From 30% RH to 90% RH, oxygen diffusivity increases by three times and interfacial resistance to oxygen
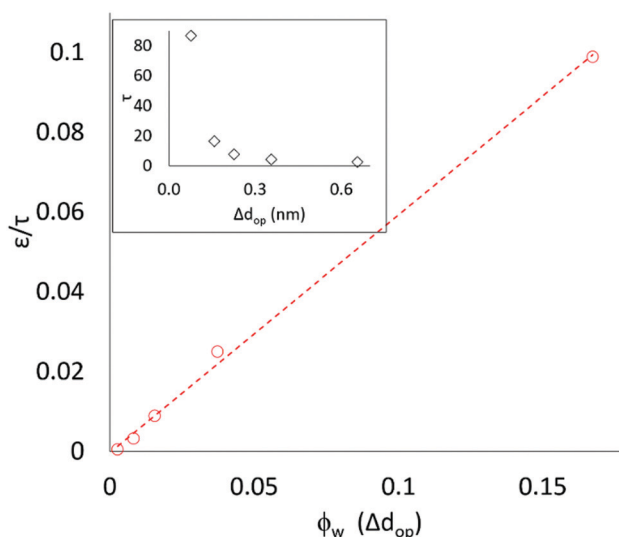

Fig. 7 Comparison between structural factors and product of water volume fraction and domain expansion; inset shows tortuosity against domain expansion.

Table 1 Comparison of oxygen transport resistance across the Nafion thin film coated on Pt and domain size in the OP and IP directions

| RH (%) | O$_2$ diffusion at 40 °C[13] | | d-Spacing [this work] | |
	Inner resistivity (10^{14} s m Pa mol^{-1})	Interfacial resistance (10^6 s m^2 Pa mol^{-1})	d_{OP} (nm)	d_{IP} (nm)
30	3.4	10	2.55	—
40	—	—	2.6	—
60	1.9	8.8	2.7	3.2
90	1.1	7.8	3.2	3.6

transport decreases by 20%.[13] Bulk oxygen diffusion resistance should be related to bulk microstructure and interfacial resistance should be related to near interface structure. Oxygen is transported through two pathways: (a) free volume in the backbone and (b) hydrophilic domains. It is evident from the data on hydrophilic domain size that an increase in oxygen diffusivity must be the result of hydrophilic domain expansion (see Table 1). Similarly, as the Pt–ionomer interface hydrates, the free volume near the interface increases, which results in lower interfacial resistance for oxygen transport. However, the layer at the free interface or the surface layer remains hydrophobic, meaning water cannot easily breakthrough the hydrophobic backbone, which raises the question of how oxygen is transported at the free interface?

VI. Conclusions

Simultaneous measurements of swelling by ellipsometry and mass uptake by QCM on a ∼55 nm thin film of Nafion on a Pt substrate yielded comparable water volume fractions, yet a finite difference between the two measurements was found through repeatable measurements on separate samples. The origin of this difference remains unresolved but serves as a cautionary note for other researchers that an error may exist when determining water content of ionomer thin films by one of these two methods. The correlation between microscopic hydrophilic domain expansion determined from GISAXS and macroscopic swelling in the OP direction yielded non-affine behaviour of thin films on Pt. The origin of non-affine behaviour is attributed to the water distribution within the ionomer thin film, evidence of which was provided by RH-dependent water distribution determined by NR.

The proton conductivity-water uptake of the ionomer thin film on Pt was analysed in terms of structural parameters: water volume fraction and domain size. In the vehicular transport-dominated regime ($\phi_w < 0.2$), we found that the tortuosity of ionomers is inversely proportional to the hydrophilic domain size. Furthermore, implications of RH-dependent water distribution from NR and hydrophilic domain size on oxygen diffusion and ORR activity were discussed. In bulk ionomers, increase in domain size very well relates with increase in oxygen diffusivity with RH. Similarly increase in free volume with RH at the Pt–ionomer interface could be the underlying cause of the increase in oxygen diffusivity with RH at the Pt–ionomer interface. In addition, increase in water content at the Pt–ionomer interface with RH also promotes desorption of sulfonic groups, thereby increasing ORR activity at the Pt–ionomer interface.

Conflicts of interest

The authors declare no conflict of interests.

References

1 M. S. Wilson and S. Gottesfeld, Thin-film catalyst layers for polymer electrolyte fuel cell electrodes, *J. Appl. Electrochem.*, 1992, **22**, 1–7.

2 Q. Luo, H. Zhang, J. Chen, P. Qian and Y. Zhai, Modification of Nafion Membrane Using Interfacial Polymerization for Vanadium Redox Flow Battery Applications, *J. Membr. Sci.*, 2008, **311**, 98–103.

3 C. D. Feng, S. L. Sun, H. Wang, C. U. Segre and J. R. Stetter, Humidity Sensing Properties of Nafion and Sol-gel Derived SiO$_2$/Nafion Composite Thin Films, *Sens. Actuators, B*, 1997, **40**, 217–222.

4 S. A. Grigoriev, V. I. Porembsky and V. N. Fateev, Pure Hydrogen Production by PEM Electrolysis for Hydrogen Energy, *Int. J. Hydrogen Energy*, 2006, **31**, 171–175.

5 K. Karan, Interesting Facets of Surface, Interfacial, and Bulk Characteristics of Perfluorinated Ionomer Films, *Langmuir*, 2019, **35**(42), 13489–13520.

6 K. Karan, Recent Advances in Materials, Microstructural Characterization, and Modeling. Current Opinions in, *Electrochemistry*, 2017, **5**, 27–35.

7 Y. Sone, P. Ekdunge and D. Simonsson, Proton Conductivity of Nafion 117 as Measured by a Four-electrode AC Impedance Method, *J. Electrochem. Soc.*, 1996, **143**, 1254–1259.

8 T. A. Zawodzinski, C. Derouin, S. Radzinski, R. J. Sherman, V. T. Smith, T. E. Springer and S. Gottesfeld, Water Uptake by and Transport Through Nafion® 117 Membranes, *J. Electrochem. Soc.*, 1993, **140**, 1041–1047.

9 K. C. Neyerlin, W. Gu, J. Jorne, A. Clark and H. A. Gasteiger, Cathode catalyst utilization for the ORR in a PEMFC analytical model and experimental validation, *J. Electrochem. Soc.*, 2007, **154**, B279–B287.

10 D. Chen, A. Kongkanand and J. Jorne, Proton Conduction and Oxygen Diffusion in Ultra-Thin Nafion Films in PEM Fuel Cell: How Thin?, *J. Electrochem. Soc.*, 2019, **166**, F24–F33.

11 A. Kusoglu and A. Z. Weber, New Insights into Perfluorinated Sulfonic-acid Ionomers, *Chem. Rev.*, 2017, **117**, 987–1104.

12 K. A. Mauritz and R. B. Moore, State of understanding of Nafion, *Chem. Rev.*, 2004, **104**, 4535–4586.

13 K. Kudo, R. Jinnouchi and Y. Morimoto, Humidity and temperature dependences of oxygen transport resistance of Nafion thin film on platinum electrode, *Electrochim. Acta*, 2016, **209**, 682–690.

14 V. Ozhukil Kollath, Y. Liang, F. D. Mayer, X. Ma, C. Korzeniewski and K. Karan, Model-Based Analyses of Confined Polymer Electrolyte Nanothin Films Experimentally Probed by Polarized ATR–FTIR Spectroscopy, *J. Phys. Chem. C*, 2018, **122**, 9578–9585.

15 Y. Nagao, Highly oriented sulfonic acid groups in a Nafion thin film on Si substrate, *J. Phys. Chem. C*, 2013, **117**, 3294–3297.

16 K. A. Page, A. Kusoglu, C. M. Stafford, S. Kim, R. J. Kline and A. Z. Weber, Confinement-driven increase in ionomer thin-film modulus, *Nano Lett.*, 2014, **14**, 2299–2304.

17 D. K. Paul, A. Fraser and K. Karan, Towards the understanding of proton conduction mechanism in PEMFC catalyst layer: Conductivity of adsorbed Nafion films, *Electrochem. Commun.*, 2011, **13**, 774–777.

18 D. K. Paul, R. McCreery and K. Karan, Proton transport property in supported Nafion nanothin films by electrochemical impedance spectroscopy, *J. Electrochem. Soc.*, 2014, **161**, F1395–F1402.

19 D. K. Paul and K. Karan, Conductivity and wettability changes of ultrathin Nafion films subjected to thermal annealing and liquid water exposure, *J. Phys. Chem. C*, 2014, **118**, 1828–1835.

20 H. K. Shim, D. K. Paul and K. Karan, Resolving the contradiction between anomalously high water uptake and low conductivity of nanothin Nafion films on SiO_2 substrate, *Macromolecules*, 2015, **48**, 8394–8397.

21 A. Kusoglu, T. J. Dursch and A. Z. Weber, Nanostructure/ Swelling Relationships of Bulk and Thin-Film PFSA Ionomers, *Adv. Funct. Mater.*, 2016, **26**, 4961–4975.

22 A. Kongkanand, Interfacial water transport measurements in Nafion thin films using a quartz-crystal microbalance, *J. Phys. Chem. C*, 2011, **115**, 11318–11325.

23 Y. Ono and Y. Nagao, Interfacial structure and proton conductivity of Nafion at the Pt-deposited surface, *Langmuir*, 2015, **32**, 352–358.

24 C. Zhang, M. Davies and K. Karan, Probing interfacial interactions of Nafion ionomer: Thermal expansion of Nafion thin films on substrates of different hydrophilicity/hydrophobicity, *J. Polym. Sci., Part B: Polym. Phys.*, 2019, **57**, 343–352.

25 S. C. DeCaluwe, P. A. Kienzle, P. Bhargava, A. M. Baker and J. A. Dura, Phase segregation of sulfonate groups in Nafion interface lamellae, quantified via neutron reflectometry fitting techniques for multi-layered structures, *Soft Matter*, 2014, **10**, 5763–5776.

26 S. C. DeCaluwe, A. M. Baker, P. Bhargava, J. E. Fischer and J. A. Dura, Structure-property relationships at Nafion thin-film interfaces: thickness effects on hydration and anisotropic ion transport, *Nano Energy*, 2018, **46**, 91–100.

27 A. Kusoglu, D. Kushner, D. K. Paul, K. Karan, M. A. Hickner and A. Z. Weber, Impact of Substrate and Processing on Confinement of Nafion Thin Films, *Adv. Funct. Mater.*, 2014, **24**, 4763–4774.

28 M. Tesfaye, D. I. Kushner and A. Kusoglu, Interplay between Swelling Kinetics and Nanostructure in Perfluorosulfonic Acid Thin-Films: Role of Hygrothermal Aging, *ACS Appl. Polym. Mater.*, 2019, **1**(4), 631–635.

29 M. Tesfaye, A. N. MacDonald, P. Dudenas, A. Kusoglu and A. Z. Weber, Exploring substrate/ionomer interaction under oxidizing and reducing environments, *Electrochem. Commun.*, 2018, **87**, 86–90.

30 D. I. Kushner, A. Kusoglu, N. J. Podraza and M. A. Hickner, Substrate-Dependent Molecular and Nanostructural Orientation of Nafion Thin Films, *Adv. Funct. Mater.*, 2019, 1902699.

31 J. A. Dura, V. S. Murthi, M. Hartman, S. K. Satija and C. F. Majkrzak, Multilamellar Interface Structures in Nafion, *Macromolecules*, 2009, **42**, 4769–4774.

32 S. Ueda, S. Koizumi, A. Ohira, S. Kuroda and H. Frielinghaus, Grazing-incident Neutron Scattering to Access Catalyst for Polymer Electrolyte Fuel Cell, *Phys. B*, 2018, **551**, 309–314.

33 U. N. Shrivastava, H. Fritzsche and K. Karan, Interfacial and Bulk Water in Ultrathin Films of Nafion, 3M PFSA, and 3M PFIA Ionomers on a Polycrystalline Platinum Surface, *Macromolecules*, 2018, **51**, 9839–9849.

34 Y. Ogata, D. Kawaguchi, N. L. Yamada and K. Tanaka, Multistep thickening of Nafion thin films in water, *ACS Macro Lett.*, 2013, **2**, 856–859.

35 I. Yagi, K. Inokuma, K. I. Kimijima and H. Notsu, Molecular Structure of Buried Perfluorosulfonated Ionomer/Pt Interface Probed by Vibrational Sum Frequency Generation Spectroscopy, *J. Phys. Chem. C*, 2014, **118**, 26182–26190.

36 K. D. Kreuer and G. Portale, A Critical Revision of the Nanomorphology of Proton Conducting Ionomers and Polyelectrolytes for Fuel Cell Applications, *Adv. Funct. Mater.*, 2013, **23**, 5390–5397.

37 T. A. Harroun, H. Fritzsche, M. J. Watson, K. G. Yager, O. M. Tanchak, C. J. Barrett and J. Katsaras, Variable Temperature, Relative Humidity (0–100%), and Liquid Neutron Reflectometry Sample Cell Suitable for Polymeric and Biomimetic Materials, *Rev. Sci. Instrum.*, 2005, **76**, 065101.

38 K. Vegso, P. Siffalovic, M. Weis, M. Jergel, M. Benkovicova, E. Majkova, L. Chitu, Y. Halahovets, S. Luby, I. Capek and

A. Satka, *In situ* GISAXS monitoring of Langmuir nanoparticle multilayer degradation processes induced by UV photolysis, *Phys. Status Solidi A*, 2011, **208**, 2629–2634.

39 T. Kawamoto, M. Aoki, T. Kimura, T. Mizusawa, N. L. Yamada, J. Miyake, K. Miyatake and J. Inukai, In-plane distribution of water inside Nafion® thin film analyzed by neutron reflectivity at temperature of 80 °C and relative humidity of 30–80% based on 4-layered structural model, *Jpn. J. Appl. Phys.*, 2019, **58**, SIID01.

40 J. Tang, W. Yuan, J. Zhang, H. Li and Y. Zhang, Evidence for a crystallite-rich skin on perfluorosulfonate ionomer membranes, *RSC Adv.*, 2013, **3**, 8947–8952.

41 M. Bass, A. Berman, A. Singh, O. Konovalov and V. Freger, Surface-induced micelle orientation in Nafion films, *Macromolecules*, 2011, **44**, 2893–2899.

42 P. Choi, N. H. Jalani and R. Datta, Thermodynamics and proton transport in Nafion II. Proton diffusion mechanisms and conductivity, *J. Electrochem. Soc.*, 2005, **152**, E123–E130.

43 C. C. De Araujo, K. D. Kreuer, M. Schuster, G. Portale, H. Mendil-Jakani, G. Gebel and J. Maier, Poly(p-phenylene sulfone)s with high ion exchange capacity: ionomers with unique microstructural and transport features, *Phys. Chem. Chem. Phys.*, 2009, **11**, 3305–3312.

44 K. D. Kreuer, On the development of proton conducting polymer membranes for hydrogen and methanol fuel cells, *J. Membr. Sci.*, 2001, **185**, 29–39.

45 K. Kodama, R. Jinnouchi, T. Suzuki, H. Murata, T. Hatanaka and Y. Morimoto, Increase in Adsorptivity of Sulfonate Anions on Pt(111) Surface with Drying of Ionomer, *Electrochem. Commun.*, 2013, **36**, 26–28.